

Supporting Information

Directed Gas-Phase Synthesis of Triafulvene under Single-Collision Conditions

Aaron M. Thomas, Long Zhao, Chao He, Galiya R. Galimova, Alexander M. Mebel, and Ralf I. Kaiser**

anie_201908039_sm_miscellaneous_information.pdf

Table S1. Peak velocities (v_p) and speed ratios (S) of the methylidyne (CH), d₁-methylidyne (CD), allene (H₂CCCH₂), d₄-allene (D₂CCCD₂), methylacetylene (CH₃CCH), and d₄-methylacetylene (CD₃CCD), d₃-methylacetylene (CD₃CCH), and d₁-methylacetylene (CH₃CCD) beams along with the corresponding collision energies (E_C) and center-of-mass angles (Θ_{CM}).

Beam	v_p (m s ⁻¹)	S	E_C (kJ mol ⁻¹)	Θ_{CM} (degree)
CH (X ² Π)	1774 ± 14	10.5 ± 0.7	18.6 ± 0.3	54.2 ± 0.4
H ₂ CCCH ₂ (X ¹ A ₁)	800 ± 10	12.0 ± 0.4		
CH (X ² Π)	1779 ± 13	12.3 ± 1.2	18.7 ± 0.2	54.2 ± 0.4
CH ₃ CCH (X ¹ A ₁)	800 ± 10	12.0 ± 0.4		
CH (X ² Π)	1713 ± 24	9.7 ± 0.5	17.8 ± 0.4	57.4 ± 0.5
CD ₃ CCD (X ¹ A ₁)	790 ± 10	12.0 ± 0.4		
D ₂ CCCD ₂ (X ¹ A ₁)	790 ± 10	12.0 ± 0.4		
CD (X ² Π)	1768 ± 9	13.1 ± 1.2	19.3 ± 0.2	52.4 ± 0.4
H ₂ CCCH ₂ (X ¹ A ₁)	800 ± 10	12.0 ± 0.4		
CD ₃ CCH (X ¹ A ₁)	790 ± 10	12.0 ± 0.4		
CH ₃ CCD (X ¹ A ₁)	800 ± 10	12.0 ± 0.4		

Table S2. Product branching ratios of the CH + methylacetylene and CH + allene reactions calculated for single-collision conditions using RRKM theory at the collision energy of 19 kJ mol⁻¹.

CH + methylacetylene					
	vinylacetylene (p1) + H	butatriene (p2) + H	triafulvene (p3) + H	C ₂ H ₂ + C ₂ H ₃	
triple bond addition	18.39%	14.55%	66.90%	0.17%	
sp ³ CH bond insertion	97.57%	0.22%	0.00%	2.42%	
sp CH bond insertion	47.01%	52.64%	0.15%	0.20%	
CC bond insertion	99.30%	0.00%	0.00%	0.69%	
CH + allene					
	vinylacetylene (p1) + H	butatriene (p2) + H	triafulvene (p3) + H	C ₂ H ₂ + C ₂ H ₃	C ₂ H ₄ + C ₂ H
double bond addition	98.58%	1.26%	0.08%	0.08%	0.00%
sp ² CH bond insertion	16.75%	0.00%	0.00%	83.18%	0.07%

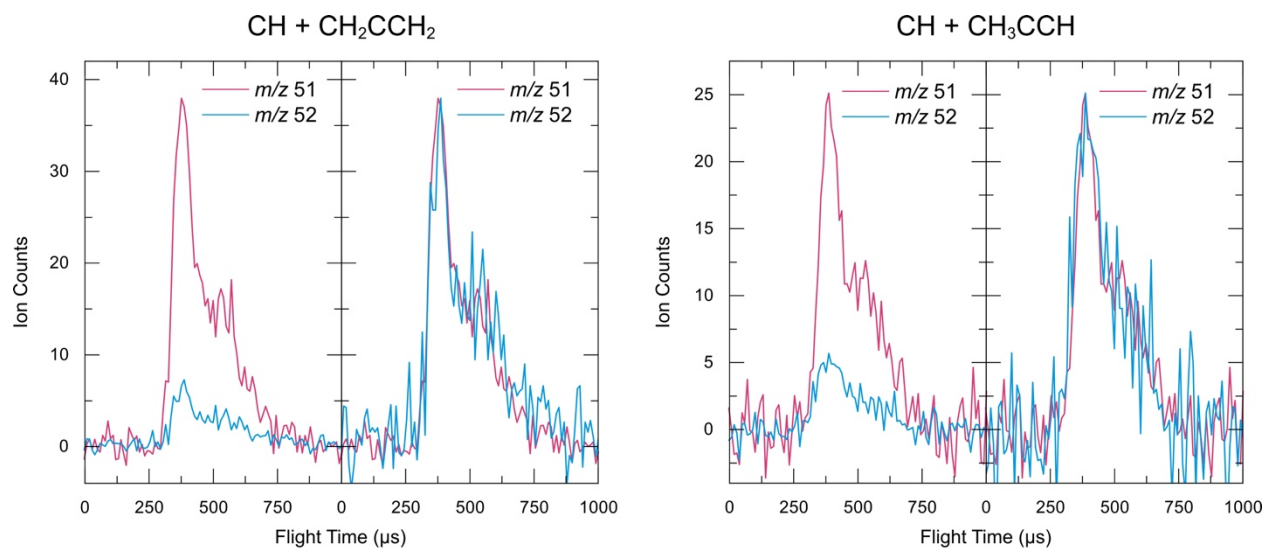


Figure S1. Time-of-flight spectra recorded at the CM angles for $m/z = 51$ (C_4H_3^+) and $m/z = 52$ (C_4H_4^+) for the reaction of the methylidyne radical (CH) with a) allene (CH_2CCH_2) and b) methylacetylene (CH_3CCH). The left and right panels depict raw and scaled TOF spectra, respectively. Since both traces overlap, signal at $m/z = 51$ represents a fragment of $m/z = 52$.

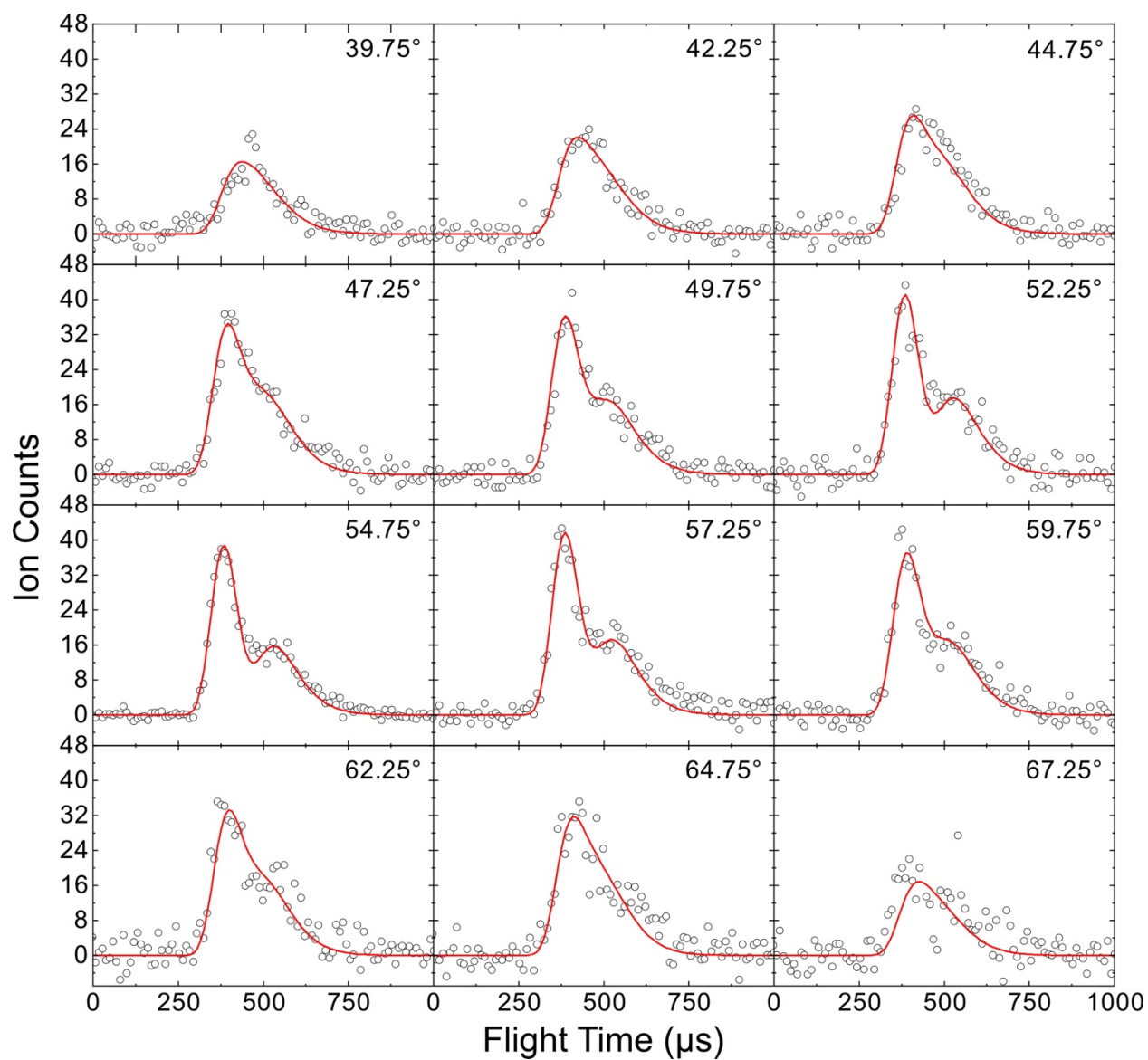


Figure S2. Time-of-flight spectra recorded at $m/z = 51$ (C_4H_3^+) for the reaction of the methylidyne radical (CH) with allene (CH_2CCH_2). The circles represent the experimental data and the solid lines the best fits.

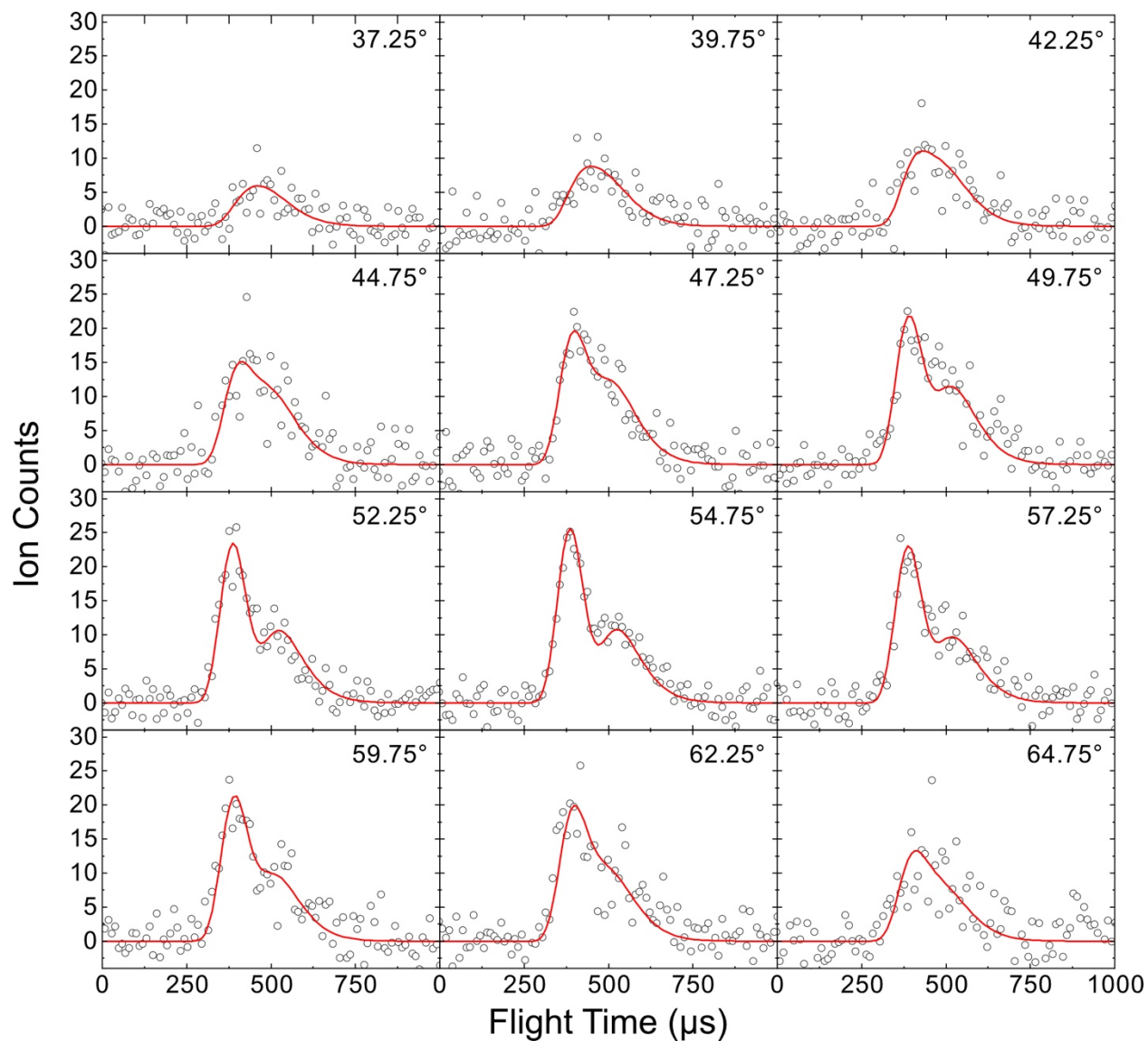


Figure S3. Time-of-flight spectra recorded at $m/z = 51$ (C_4H_3^+) for the reaction of the methylidyne radical (CH) with methylacetylene (CH_3CCH). The circles represent the experimental data and the solid lines the best fits.

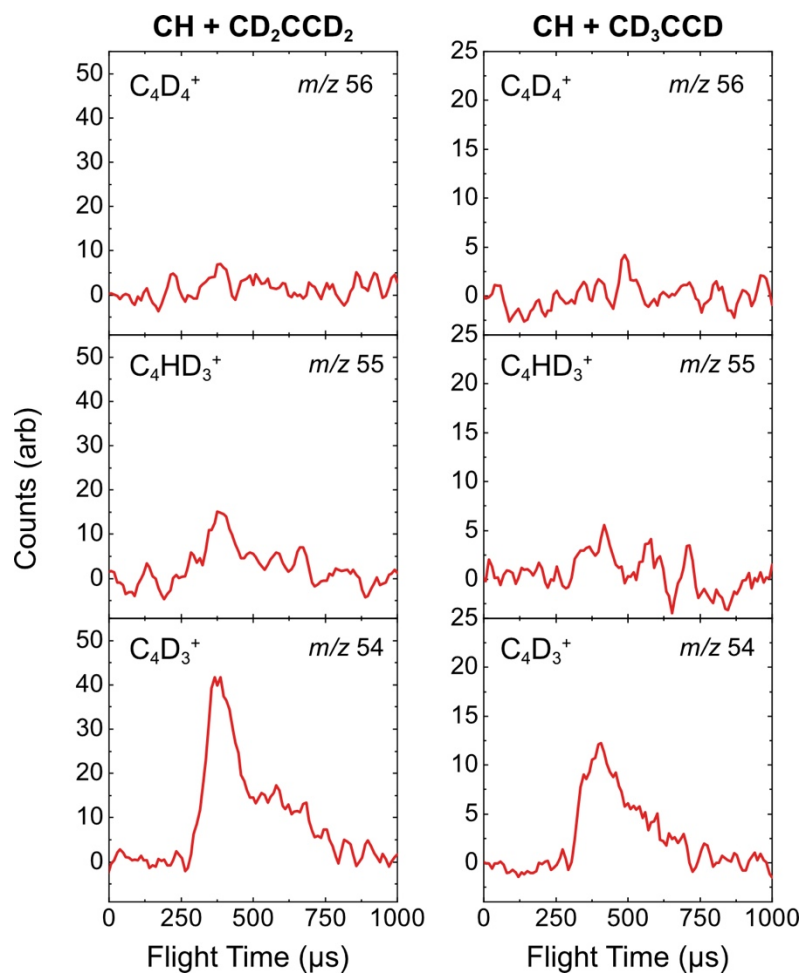


Figure S4. Time-of-flight (TOF) spectra at recorded at *m/z* 56, 55, and 54 for the reactions of the methylidyne (CH) radical with (*left*) d₄-allene (CD₂CCD₂) and (*right*) d₄-methylacetylene (CD₃CCD).

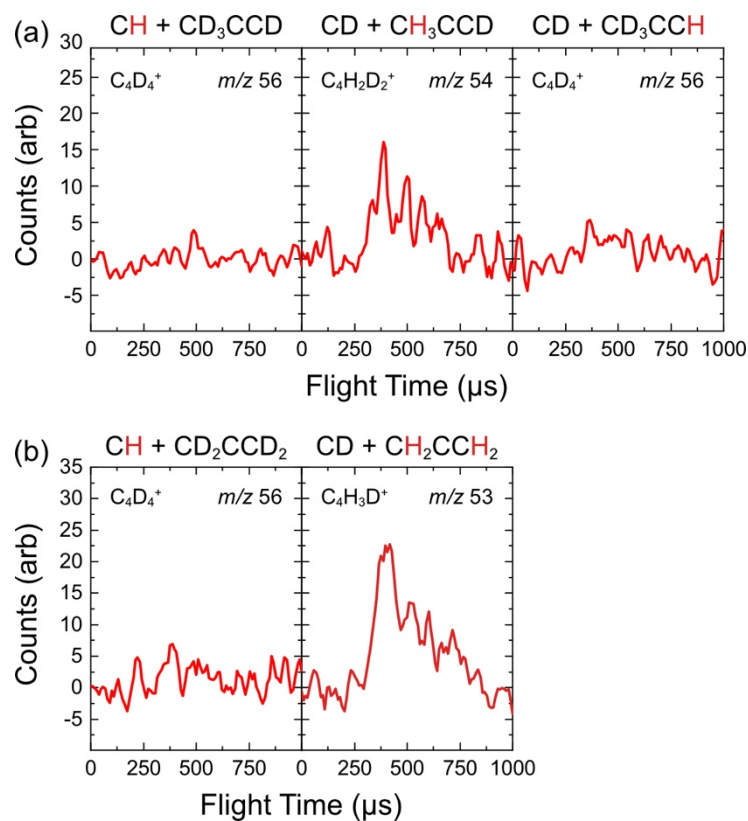


Figure S5. Time-of-flight (TOF) spectra recorded at mass-to-charge (m/z) ratios corresponding to the singly-ionized hydrogen-loss product formed in the partially deuterated reactions of (a) CH plus methylacetylene (CH_3CCH) and (b) CH plus allene (CH_2CCH_2) reactions. Ion counts at $m/z = 56$ for the CD/ CD_3CCH system can be accounted by ^{13}C isotopes and hence $^{13}\text{CC}_3\text{D}_3\text{H}$.

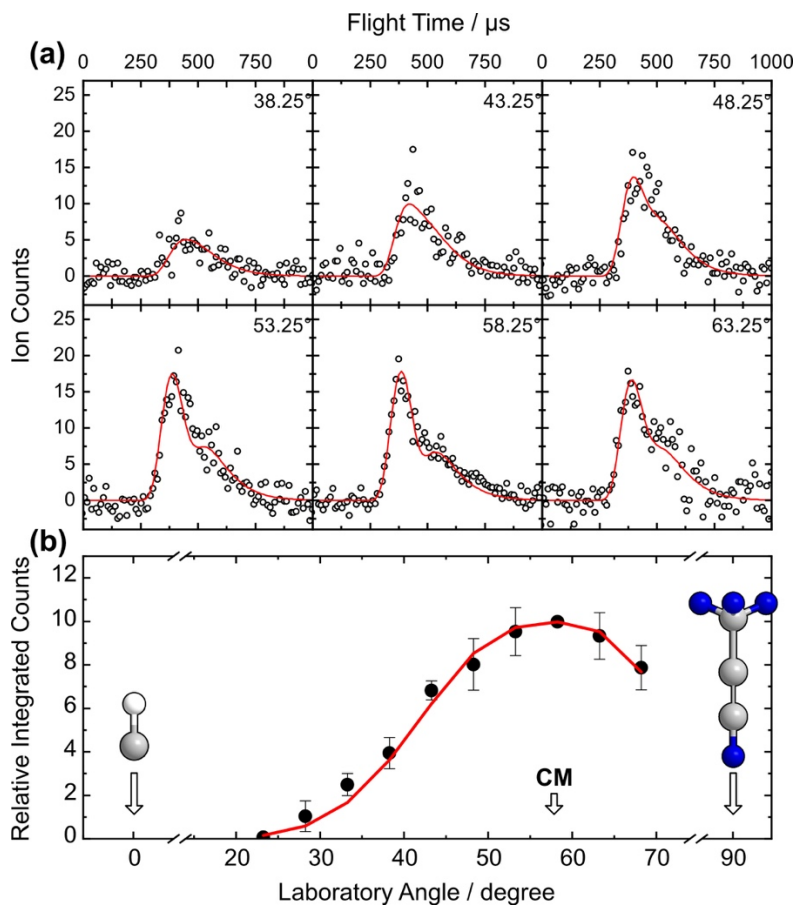


Figure S6. After establishing the source of the deuterium loss in the $\text{CH} + \text{CD}_3\text{CCD}$ reaction, we collected time-of-flight (TOF) spectra at m/z 54 (C_4D_3^+) in 5° intervals in the laboratory frame to further constrain the deuterium-loss channel for comparison with the data obtained in the fully hydrogenated reaction. The resulting laboratory angular distribution is symmetric about the CM angle of $57.4 \pm 0.5^\circ$ and is otherwise similar to those obtained from the $\text{CH} + \text{H}_2\text{CCCH}_2$ and $\text{CH} + \text{CH}_3\text{CCH}$ systems at m/z 51. a) TOF spectra and b) laboratory angular distribution recorded at m/z 54 (C_4D_3^+) for the reaction of the methylidyne radical with d_4 -methylacetylene. The circles represent the experimental data and the solid lines the best fits.

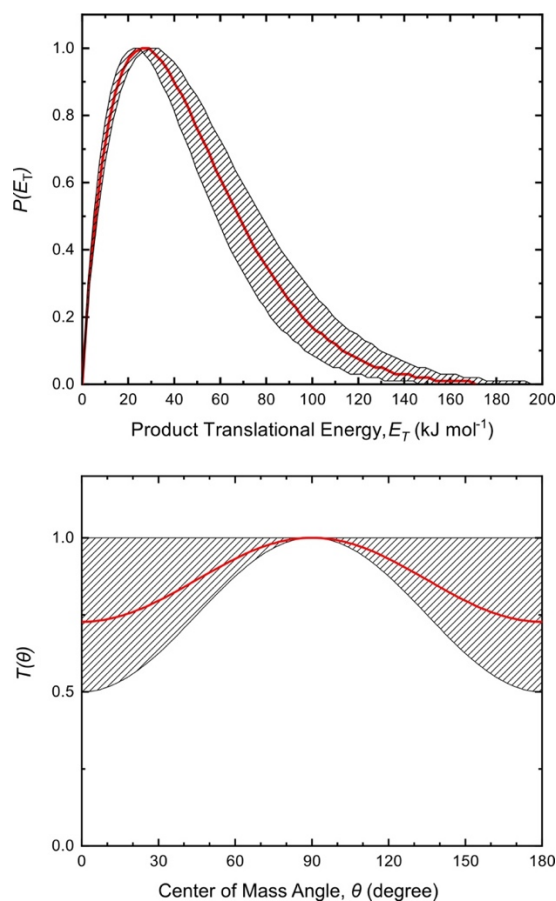


Figure S7. The CH + CD₃CCD system was fit with parameters similar to those used for the CH + CH₃CCH and CH + H₂CCCH₂ systems. The $P(E_T)$ peaks at 28 ± 4 kJ mol⁻¹, extends out to 171 ± 25 kJ mol⁻¹, and has an average E_T of 46 ± 7 kJ mol⁻¹. The C₄HD₃ molecules formed in this reaction by atomic deuterium emission are therefore characterized by a reaction exoergicity of 153 ± 25 kJ mol⁻¹. The $T(\theta)$ portrays product flux at all angles and is forward-backward symmetric with a maximum at 90°. Hence, we draw similar conclusions regarding the CH + CD₃CCD → C₄HD₃ + D reaction coordinate, namely the involvement of relatively long-lived bound intermediates decomposing via tight exit transition states. a) center-of-mass translational energy $P(E_T)$ and b) angular $T(\theta)$ flux distributions for the reaction of the methylidyne radical with methylacetylene-d₄ forming C₄HD₃ isomer(s) by atomic deuterium emission. Solid lines represent the best fit while shaded areas indicate the experimental error limits.